Clays and Clay Minerals, Vol. 57, No. 6, 706–714, 2009.

AFM STUDY OF SMECTITES IN HYBRID LANGMUIR-BLODGETT FILMS: SAPONITE, WYOMING BENTONITE, HECTORITE, AND LAPONITE

TAMÁS SZABÓ[1,3], JUN WANG[1,4], ALEXANDER VOLODIN[2], CHRIS VAN HAESENDONCK[2], IMRE DEKANY[3], AND ROBERT A. SCHOONHEYDT[1,]

[1] Centre for Surface Chemistry and Catalysis, K.U.Leuven, Kasteelpark Arenberg 23, 3001 Leuven, Belgium
[2] Department of Physics and Astronomy, K.U. Leuven, Celestijnenlaan 200D, 3001, Leuven, Belgium
[3] Department of Colloid Chemistry, University of Szeged, Aradi Vt 1, H-6720 Szeged, Hungary
[4] Chemistry College, Huazhong Normal University, Wuhan, Hubei, China 430079

Abstract—The sizes and shapes of single clay mineral layers are difficult to determine though they are important parameters which determine the final properties of clay polymer nanocomposites and of ultrathin clay mineral films. To determine these sizes and shapes, hybrid monolayers of clay minerals (saponite, hectorite, Wyoming bentonite, and Laponite) and Rhodamine B octadecyl ester perchlorate (RhB18) were prepared using the Langmuir-Blodgett (LB) technique and studied with atomic force microscopy (AFM). The AFM images reveal monolayers of elementary clay mineral layers, which are randomly oriented and have a wide range of sizes. The layers have typical shapes: lath-like for hectorite, plates for Wyoming bentonite, a mixture of laths and plates for saponite, and aggregates of very small layers of Laponite. Two types of layers were present in the LB films of saponite, Wyoming bentonite, and hectorite in a 40:60 ratio: (1) single layers 0.96 nm thick hybridized with RhB18; and (2) particles consisting of two clay layers with an intercalated monomolecular layer of water molecules and hybridized with RhB18. The Laponite particles in the hybrid LB films consist mainly of aggregates of two and three single layers.

Key Words—AFM, Hectorite, Laponite, Saponite, Wyoming Bentonite.

INTRODUCTION

The morphology of clay mineral layers and aggregates has attracted the attention of clay researchers for many years. Beutelspacher and Van der Marel (1968) published an atlas of electron microscopy images of clay minerals and their admixtures. In the case of swelling clays or smectite, the atlas revealed aggregates of various sizes and shapes, depending on the type of clay mineral and its origin. The situation was considerably improved by the introduction of scanning electron microscopy (SEM) and, especially, atomic force microscopy (AFM). Note that, while SEM images are two-dimensional, AFM images give three-dimensional information. The excellent depth resolution of the AFM makes it possible to measure the height of the clay layers at the nanometer scale.

The scanning probe microscope technique was applied for the first time to mixed-layer illite-smectite from the North Sea by Lindgreen *et al.* (1991) who showed that scanning tunneling microscopy measurements could be performed on the very thin layers of smectites. Methods to image clay minerals in aqueous medium by AFM have also been developed (Bickmore *et al.*, 1999). Special attention has been given to the morphology and surfaces of kaolinite because of the industrial interest in this mineral (Zbik and Smart, 1998; Bickmore *et al.*, 2002).

In the case of smectite, AFM has been used in morphology studies and for estimating the edge-surface areas. Tournassat *et al.* (2003) described the irregular morphology of MX80 bentonite (Wyoming) with a lateral surface area of 7.4±0.7 m^2/g and a mean height of 1.625 nm. The height can be interpreted as a mixture of single layers surrounded by a monomolecular water layer (1.25 nm) and particles consisting of two layers with one intercalated water layer (2.2 nm). The lateral dimensions of the same MX80 bentonite fall into two populations, one with characteristic dimensions of 320−400 nm × 250 nm and a group of smaller particles, typically 60 nm × 50 nm. A synthetic montmorillonite is also characterized by two populations, but with smaller lateral dimensions: 200−250 nm × 120 nm and 53 nm × 25 nm (Cadene *et al.*, 2005). For Laponite, 80% of the particles observed using AFM consisted of single layers 1.2 nm thick (Balnois *et al.*, 2003); 20% were double layers. In those studies the substrate was atomically smooth, freshly cleaved mica. For measurements in aqueous medium the mica surface was covered with polyethyleneimine (PEI). Dilute dispersions of smectites were deposited on the mica surface and the water was allowed to evaporate.

In the Langmuir-Blodgett (LB) technique a dilute aqueous dispersion of smectite particles interacts with amphiphilic cations at the air-water interface of this clay dispersion. A hybrid monolayer of amphiphilic cations-clay layers is formed at the air-water interface by ion

* E-mail address of corresponding author:
Robert.schoonheydt@biw.kuleuven.be
DOI: 10.1346/CCMN.2009.0570604

exchange. The hybrid monolayer can be transferred to a substrate (glass, quartz, Si, ZnSe) for spectroscopic investigation and for AFM measurements (Ras *et al.*, 2007). Smectite particles and the amphiphilic cations can, therefore, be studied separately by attenuated total reflection-Fourier-transform infrared spectroscopy (ATR-FTIR), ultraviolet-visible (UV-vis) spectroscopy, and fluorescence spectroscopy (Ras *et al.*, 2003, 2004a, 2004b). In the present study the LB technique was used to produce hybrid monolayers of smectites with the octadecyl ester of rhodamine B (RhB18). These monolayers were then examined by AFM to obtain information about the sizes and shapes of the elementary layers of Laponite, hectorite, saponite, and Wyoming bentonite. Such smectites are frequently used in the preparation of clay-based polymer nanocomposites (Carrado and Bergaya, 2007) and of bio-inorganic hybrid materials (Ruiz-Hitzky *et al.*, 2008). In nanocomposites the smectites must preferably be dispersed in the (bio)polymer matrix at the single-layer level. The sizes and shapes of the single layers are fundamental properties of clay minerals which determine the final properties of the clay-based polymer nanocomposites and of the bio-inorganic hybrid materials.

EXPERIMENTAL

Materials

Saponite, hectorite, and Wyoming bentonite (WB) were obtained from the Source Clays Repository of The Clay Minerals Society (hosted at Purdue University, West Lafayette, Indiana, USA). Laponite was obtained from Laporte Inorganics (UK) and used as received. The clay minerals (saponite, hectorite, Wyoming bentonite) were Na^+ saturated by repeated exchange with 1 M NaCl solution and washing. The 0.5–2 μm particle size fraction was obtained by centrifugation. The clay minerals were stored as freeze-dried powders. Rhodamine B octadecyl ester perchlorate (= 98%, RhB18) was purchased from Sigma-Aldrich (St. Louis, Missouri) and used as received.

Preparation of hybrid monolayers

The clay mineral dispersions were prepared by dispersing 1 g of clay in 1 L of pure water. The dispersions were stirred for 24 h and subsequently diluted to 50 mg/L or 50 ppm (saponite, hectorite), 10 ppm (Wyoming bentonite), 2 ppm (Laponite), and 0.2 ppm (Laponite) and agitated in an ultrasonic bath for 30 min prior to use in the LB trough. 40 μL of an RhB18 solution in chloroform (1×10^{-3} mol/L) was spread on the air-water interface in a LB trough (NIMA611). After 30 min, the hybrid monolayers were compressed at a rate of 10 cm^2/min and the surface pressure-area isotherms recorded. The hybrid monolayer films were deposited either on quartz, Si wafer, or ZnSe substrates in the upstroke mode at a surface pressure of 15 mN/m and a dipping speed of 5 mm/min. The system was kept at 15 mN/m for 15 min, or 60 min (waiting time) prior to deposition. The standard waiting time was 15 min. After deposition, the films were not washed prior to examination by AFM and spectroscopic techniques.

Characterization techniques

The surface pressure-area isotherms and the monolayer deposition were performed in a NIMA 611 Langmuir trough. The AFM imaging was performed in air with a commercial AFM system Autoprobe M5 (Veeco Instr., Breda, The Netherlands) using silicon cantilevers with a sharp, high apex ratio tip (UltraLevers™, Veeco Instr.). All the AFM images presented here were obtained in intermittent-contact ('tapping') mode. Typical scan areas were 3 μm × 3 μm and 1 μm × 1 μm. The vertical noise level was <0.2 nm. The monolayers on oxidized Si wafer substrates were used for the AFM measurements. UV-vis spectra were recorded using a Perkin Elmer Lambda 12 apparatus. Fluorescence spectra were measured using a SPEX Fluorolog 322 fluorescence spectrometer. The fluorescence spectra were collected under 45° geometry. The excitation wavelength was 550 nm. In both cases quartz plates were used as the substrate.

RESULTS

π-A isotherms

The surface pressure-area (π-A) isotherms of RhB18 in the presence of a subphase containing 50 mg/L of clay minerals are shown (Figure 1). The isotherm of RhB18 on pure water is given for comparison. The isotherm of RhB18 on pure water corresponds with that of a typical liquid expanded state at the gas-water interface (Roberts, 1990; Ras *et al.*, 2004a). The presence of 50 mg/L of clay minerals in the subphase significantly influences

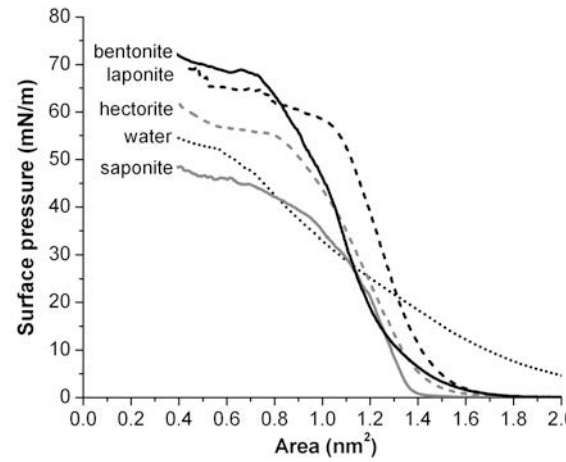

Figure 1. Surface pressure-area isotherms of RhB18 on water and aqueous clay dispersions.

https://doi.org/10.1346/CCMN.2009.0570604 Published online by Cambridge University Press

the isotherms. Firstly, the lift-off areas shift to smaller values. They are 1.40, 1.45, 1.48, and 1.35 nm^2/RhB18 molecule for saponite, hectorite, Laponite, and Wyoming bentonite, respectively, compared to 2.1 nm^2/RhB18 molecule on water. Secondly, the difference in lift-off areas for the different clay minerals is small and does not exceed the uncertainty values associated with their determination. The average value is 1.42 nm^2. Thirdly, the slopes of the isotherms in the presence of the clay minerals are greater than that of the isotherm without clay minerals (as observed previously – Ras *et al.*, 2004a, 2004b). The slopes are a measure of the compressibility of the monolayers and the RhB18 monolayers, containing clay mineral layers, are less compressible than RhB18 monolayers in the absence of clay mineral layers.

AFM measurements

The AFM images of hybrid RhB18/clay mineral monolayers deposited on a Si substrate at a surface pressure of 15 mN/m and a waiting time of 15 min are shown in Figures 2–7. The layers of saponite are clearly observed (Figure 2), forming a closely packed array of layers of various sizes and shapes. Some are plate-like, others lath-like. Many layers have irregular shape, however, especially the small ones. The largest layer in Figure 2a is ~1.4 μm × 0.6 μm. Some layers, especially those with a lath-like shape, are aligned, but overall, the orientation of the layers is random. The heights of the hybrid monolayer along the horizontal lines A, B, and C in the AFM image are shown (Figure 2a). Over the length of these lines (3 μm), the top of hybrid monolayer is at ~4 nm and the bottom at 0 nm. The latter corresponds to the black spots in Figure 2a which are due to parts of the substrate not being covered with saponite layers. The white particles in the AFM image have a height of ~8 nm. The height-distribution histogram covers the range 1–6 nm, but most saponite layers have a height of 3–4 nm, in agreement with the line analysis.

Another typical AFM image of a hybrid monolayer of RhB18/saponite (Figure 3) illustrates the effects of waiting time. The waiting time in this case, between compression and deposition, was 60 min at 15 mN/m. The same type of saponite layers as described above was noted. The number of layers per unit area is smaller than in Figure 2, however, corresponding to a surface coverage of 52%, compared to 82% in Figure 2, meaning that as the waiting time increased, a significant amount of hybridized saponite-RhB18 layers were dragged from the air-water interface into the water.

The height of the saponite monolayer along the lines A, B, and C in Figure 3 is also shown. The 4 nm height is seen again, as observed in Figure 2. The same holds for the white spots with a height of 8 nm. These heights correspond to particles consisting of several saponite layers. The height-distribution histogram in Figure 3 shows bimodal distribution, with maxima at ~1.8 nm and 3.5 nm in a ratio of ~2:3, implying that when the saponite layers were well separated in the film, two types of layers were prominent. They have charactistic heights, one being twice that of the other.

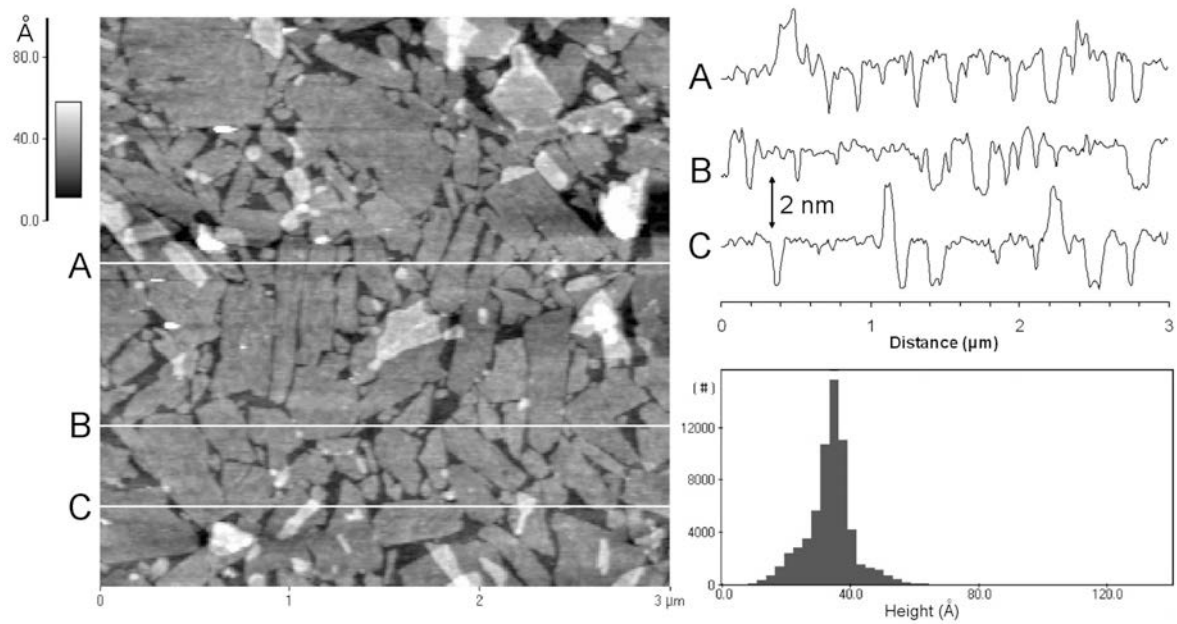

Figure 2. Left: AFM image of a RhB18/saponite monolayer (waiting time: 15 min); upper right: height analysis of the RhB18/saponite monolayer along the horizontal lines A, B, and C; lower right: height-profile histogram.

https://doi.org/10.1346/CCMN.2009.0570604 Published online by Cambridge University Press

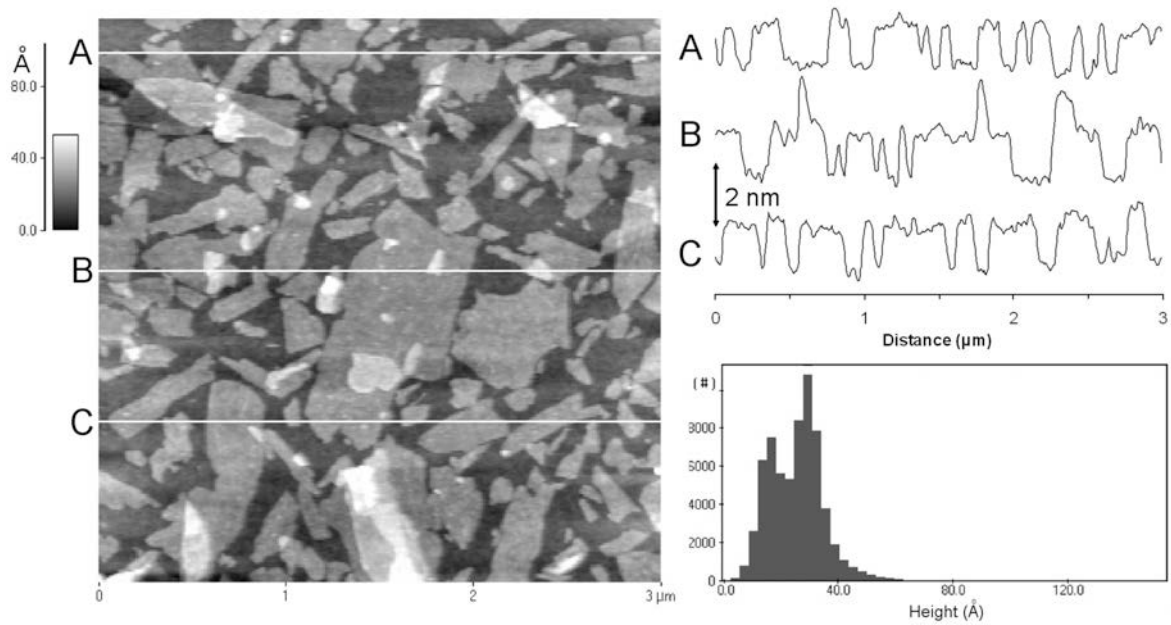

Figure 3. Left: AFM image of RhB18/saponite monolayer (waiting time: 60 min); upper right: height profiles of the RhB18/saponite monolayer along the horizontal lines A, B, and C; lower right: height-distribution histogram.

Typical 3 µm × 3 µm images of a LB film of Laponite (Figure 4), prepared from a 2 ppm dispersion, revealed a continuous two-dimensional film of Laponite layers with almost grayish image contrast. The small dark spots, scattered over the image, are indicative of empty spaces, *i.e.* the bare substrate. The white spots indicate vertical aggregation of Laponite particles. Individual Laponite particles are difficult/impossible to distinguish clearly, consistent with the height analysis along the horizontal lines, A, B, and C. Along line A, from left to right, is a continuous grayish background 4–6 nm thick, except for the upper image, where it is 2–4 nm thick. As before, where the line crosses a black hole the height drops to zero (corresponding to the bare substrate) and where it crosses particles, heights of 8 nm and in one case ~13 nm were recorded, corresponding to

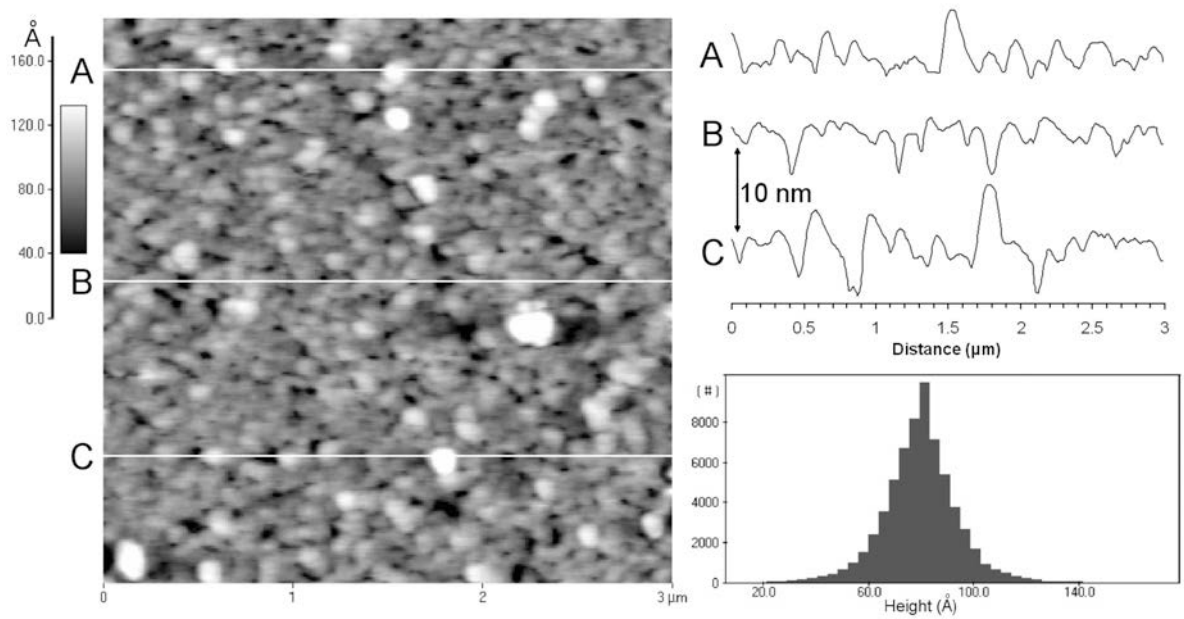

Figure 4. AFM image of RhB18/Laponite monolayers, prepared from 2 ppm dispersions (left). Upper right: height analyses along the horizontal lines A, B, and C; lower right: height-distribution histogram.

https://doi.org/10.1346/CCMN.2009.0570604 Published online by Cambridge University Press

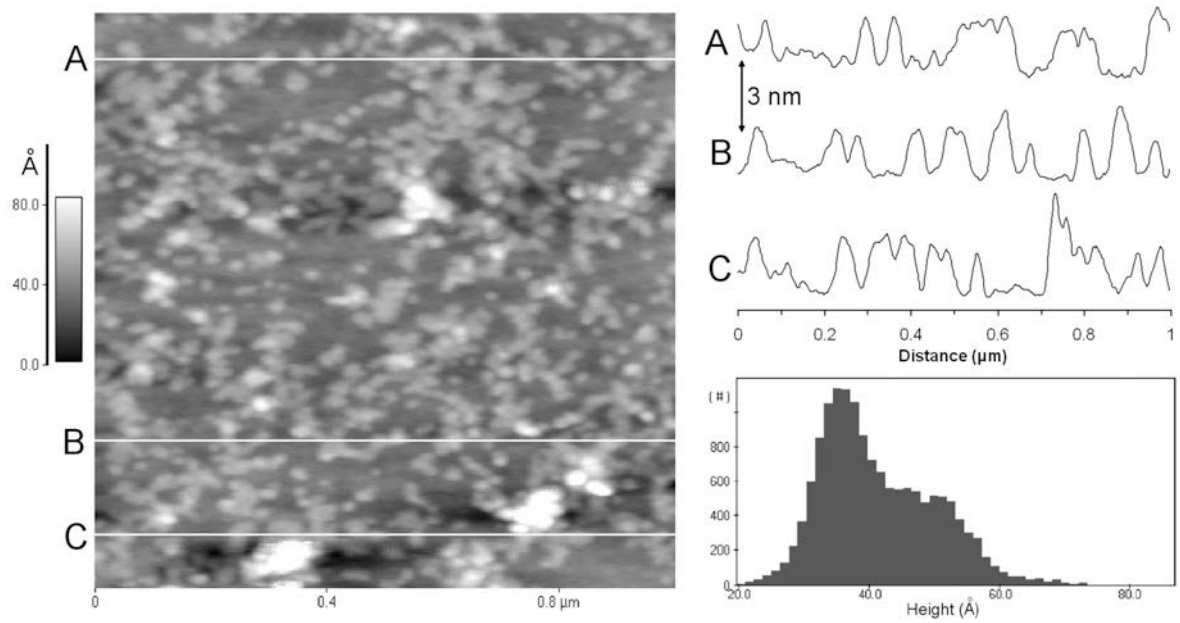

Figure 5. Left: AFM image of RhB18/laponite monolayers, prepared from 0.2 ppm dispersions. Upper right: height analyses along the horizontal lines A, B, and C; lower right: height-distribution histogram.

aggregates of Laponite layers. The height-distribution histogram has an almost symmetrical shape with maximum at ~8 nm.

To obtain a better separation between the individual Laponite layers, LB films were prepared from 0.2 ppm Laponite dispersions. Typical AFM images (Figure 5) revealed light-gray regions with two-dimensional aggregation of individual Laponite layers and white spots, indicative of vertical aggregation, as the most prominent features. A few individual Laponite layers scattered over the bare substrate are also noted, at a size of ~20 nm. Analysis of the height fluctuations along lines A, B, and C in Figure 5 reveals that most particles are 2–3 nm high. The white spots, typical of vertical aggregation, are 4 nm or more in height. The height-distribution histogram is bimodal with maxima at ~3.5 nm and 5 nm

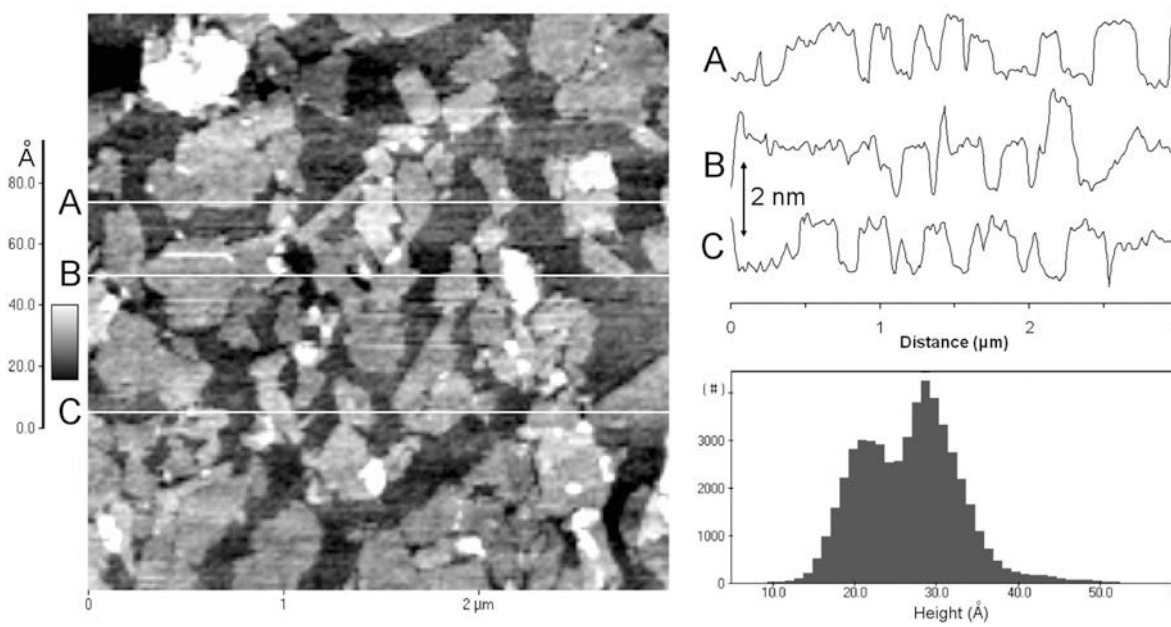

Figure 6. Left: AFM image of an RhB18/Wyoming bentonite monolayer. Upper right: height analysis along the horizontal lines A, B, and C; lower right: height-distribution histogram.

https://doi.org/10.1346/CCMN.2009.0570604 Published online by Cambridge University Press

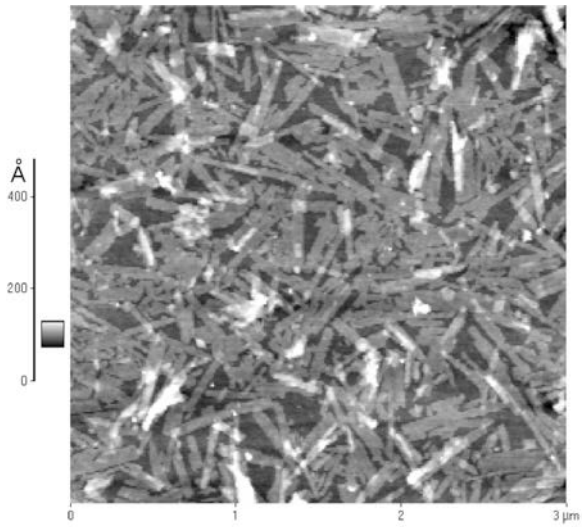

Figure 7. AFM image (3 µm × 3 µm) of RhB18/hectorite monolayer.

with about two-thirds of the Laponite layers in the 3.5 nm category.

Typical images of LB films prepared from 10 ppm Wyoming bentonite (WB) dispersions (Figure 6) reveal the presence of well separated, irregularly shaped, and randomly oriented layers of various sizes. The height analysis along the horizontal line in Figure 6 reveals heights of 1.5−2.1 nm. The topographical features which appear as white spots have heights of 3−4 nm and lateral dimensions which are smaller than those of the single WB layers. The white spots suggest: (1) very small fractions of WB layers were attached to larger ones; or (2) dust particles were present on large, single layers of Wyoming bentonite. Explanation 1 is more likely because white spots appeared in each LB film, irrespective of the preparation conditions. The height-distribution histogram was bimodal with maxima at 2.1 and 3 nm, most Wyoming layers belonging to the 3 nm category.

Finally, the AFM images of the hybrid monolayer of RhB18/hectorite (Figures 7 and 8) showed that all the particles were lath-like and their lengths varied considerably. The largest lath in the image is ~1 µm × 0.08 µm. The surface coverage in the film is 72%. The lath-like particles were randomly oriented and some overlap, as demonstrated by the occurrence of white spots in the AFM image. The heights of the layer along the lines A, B, and C in Figure 8 are also shown. The layer is 2 − 2.5 nm thick. At one point two layers are overlapping. The measured thickness was 4.5 nm in that case. The height-distribution histogram shows a bimodal distribution with maxima of 2.1 and 3 nm, the latter being far more abundant than the former.

Spectroscopy

The presence of RhB18 molecules hybridized with clay mineral layers in the LB monolayers was confirmed by absorption and fluorescence spectroscopy. The absorption maxima of RhB18 fall in the range 571−581 nm (Figure 9). A small red shift was observed in the maxima of the RhB18 spectra in the presence of clay mineral layers with respect to the position of the absorption maximum in a monolayer without clay

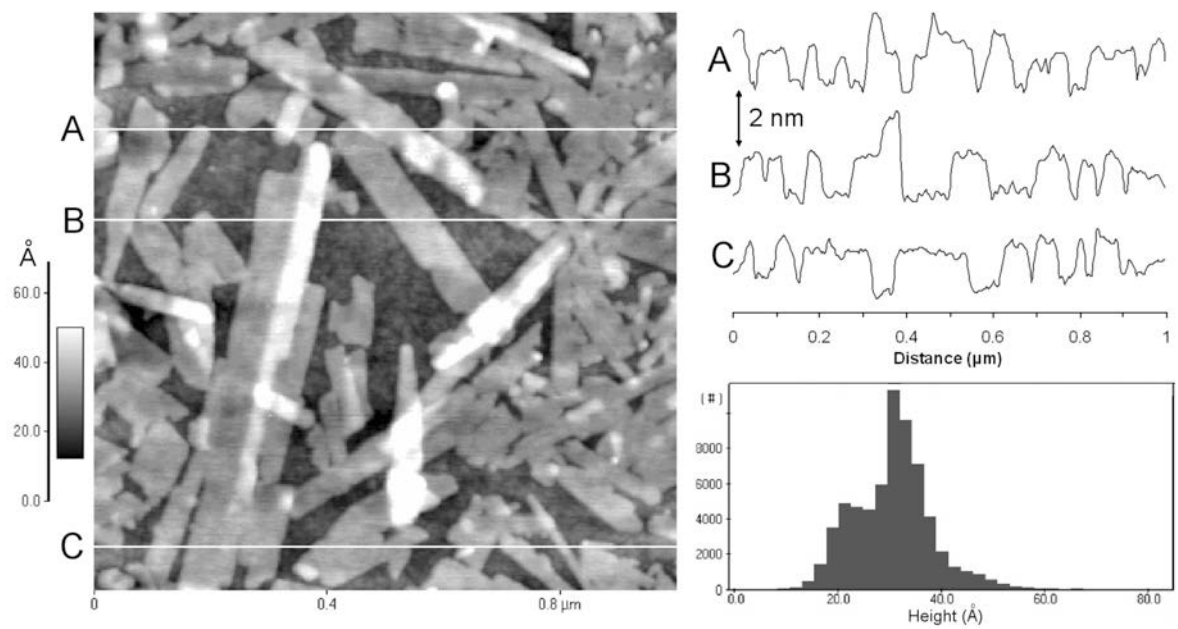

Figure 8. Left: AFM image (1 µm × 1 µm) of an RhB18/hectorite monolayer. Upper right: height profiles along the horizontal lines A, B, and C; lower right: height-distribution histogram.

https://doi.org/10.1346/CCMN.2009.0570604 Published online by Cambridge University Press

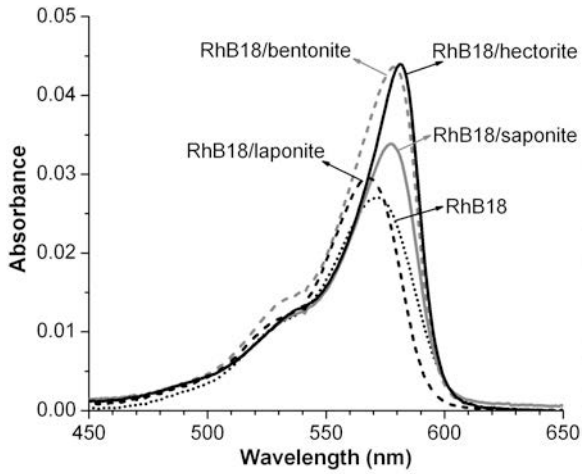

Figure 9. UV-vis spectra of an RhB18 monolayer and hybrid monolayers: RhB18/laponite, RhB18/saponite, RhB18/Wyoming bentonite, and RhB18/hectorite.

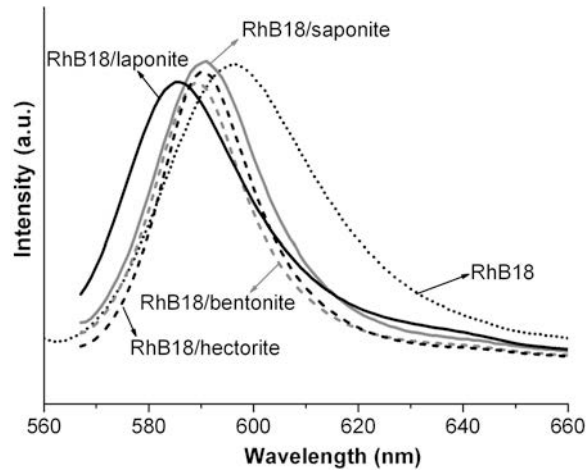

Figure 10. Emission spectra of monolayers of RhB18, RhB18/laponite, RhB18/saponite, RhB18/Wyoming bentonite, and RhB18/hectorite. The spectra have been normalized.

mineral layers, except for Laponite. The maxima of the spectra of Figure 10 (Table 1) fall in the range 586–596 nm. The fluorescence maxima of the RhB18 fluorescence in the presence of clay mineral layers are blue shifted by 6–10 nm with respect to the 596 nm for the RhB18 monolayer in the absence of clay mineral layers. The apparent Stokes' shift is defined as the difference between the maxima of the absorbance and fluorescence spectra (Table 1). The apparent Stokes' shift of RhB18 monolayers is 740 cm^{-1}; those of RhB18 hybridized with the clay layers in the LB films is 540–270 cm^{-1}, the exact value depending on the type of clay. In any case, adsorption of RhB18 cations on the clay mineral surfaces leads to systematically smaller apparent Stokes' shifts.

DISCUSSION

Surface pressure-area isotherms

The lift-off areas and the slopes of the π-A isotherms (Figure 1) indicate that the layers of the 2:1 smectites under investigation are involved in LB film formation at the air-water interface. Spectroscopy of the hybrid monolayer films (Figures 9–10) revealed small but systematic shifts of band maxima of absorption and fluorescence spectra of RhB18, indicative of the interaction of RhB18 molecules with the clay mineral surfaces (Yariv, 2001; Cenens and Schoonheydt, 1988; Bujdak, 2006). Hybrid monolayers of RhB18-elementary layers of smectites were, therefore, formed at the air-water interface with RhB18 molecules adsorbed at the surface of the clay mineral layers.

The lift-off area per RhB18 molecule in the hybrid layers is 1.42 nm^2, 0.68 nm^2 less than the lift-off area of RhB18 monolayers in the absence of clay minerals. In the former case, electrostatic attraction between the negatively charged clay mineral layers and the cationic RhB18 molecules was dominant over the repulsion between the positively charged RhB18 molecules. In the absence of clay minerals, the repulsive electrostatic interactions among the RhB18 molecules in the monolayers were dominant, giving a larger lift-off area.

The mechanism of formation of hybrid monolayers at the air-water interface is ion exchange. Cationic dyes are exchanged very selectively on smectites (Yariv and Cross, 2001; Bujdak, 2006). With RhB18 cations at the air-water interface, the elementary clay mineral layers in the subphase are attracted to the interface (against gravitational forces) to form the hybrid monolayer, which is metastable at the air-water interface. With time, the

Table 1. Spectroscopy data from different monolayers (nm).

	UV absorbance (nm)	Emission (nm)	Stokes' shift (nm cm^{-1})	
RhB18	571	596	25	740
RhB18/saponite	578	590	12	360
RhB18/laponite	568	586	18	540
RhB18/hectorite	581	590	9	270
RhB18/Wyoming	579	589	10	290

https://doi.org/10.1346/CCMN.2009.0570604 Published online by Cambridge University Press

individual hybridized layers diffuse slowly into the subphase. For saponite, with increased time between monolayer formation and transfer to the substrate, the particle density in the monolayer decreased (Figures 2, 3).

Sizes and shapes of smectite layers

The AFM images of LB films of individual layers of smectites, hybridized with RhB18 cations, reveal clearly the individual clay mineral layers, not the individual RhB18 molecules. The differences in sizes and shapes are pronounced. Hectorite layers have lath-like shapes of different lengths. Saponite consists of a mixture of lath-like and plate-like layers. Wyoming bentonite is clearly plate-like with platelets of various sizes and shapes. Individual Laponite layers are only seen if hybrid monolayers are prepared from the 0.2 ppm dispersion. They have a rounded shape with a diameter of 20–40 nm. The sizes of individual clay mineral layers can be determined if the clay mineral layers are clearly separated in the AFM image. The degree of coverage of the substrate by clay mineral layers must be relatively small; in the case of saponite this was established by increasing the waiting time before deposition from 15 to 60 min, and by decreasing the amount of clay in the subphase as for Laponite.

The height-distribution histograms reveal a bimodal distribution for the four smectites (Table 2). The natural clay minerals are characterized by height maxima of 1.8–2.1 nm and 3.0–3.5 nm with an almost equal distribution: 40% for the first and 60% for the second height. Laponite is clearly an exception with characteristic heights of 3.6 and 5.0 nm in a 65:35 ratio. The heights represent clay layers with adsorbed RhB18 molecules and, possibly, water. Two possible configurations for RhB adsorbed on Wyoming bentonite were established by Klika *et al.* (2004) and Čapková *et al.* (2004), one with a basal spacing of 1.8 nm and another with a basal spacing of 2.3 nm. The values agree well with the characteristic heights established in the present study: 1.8 and 2.1 nm. The spacings are due to a single layer of clay (0.96 nm) with one monomolecular layer of RhB18 molecules adsorbed on it. The differences between Klika's work and the present study are: (1) the C18 hydrocarbon chain on our RhB18, which is absent from RhB; (2) the water content of the LB films might be different from that in the RhB-WB systems of Klika *et al.* (2004) and Čapková *et al.* (2004). In the LB films from the present study, the water content was small or even zero (Ras *et al.*, 2003). Despite these differences the agreement is very good, indicating that the C18 alkyl chain does not contribute significantly to the height of the elementary layers.

The 3–3.5 nm heights can be explained simply by the addition of a second elementary clay layer to the RhB18 hybrid monolayer discussed above. Three situations can be envisaged. (1) The addition of a 'naked' clay layer 0.96 nm thick – this leads to characteristic particle thicknesses of 2.76–3.06 nm. (2) The addition of a hydrated clay layer 1.25 nm thick – leading to particle thicknesses of 3.05–3.35 nm. (3) Addition of a single clay layer, which is hydrated on both sides – the corresponding thickness is then ~1.5 nm. The characteristic height of the clay layers then became 3.3–3.6 nm. The experimentally obtained height of 3.0 nm for hectorite and Wyoming bentonite corresponds to the first case. The 3.5 nm of saponite is closer to the third case.

Clearly, Laponite is a special case. Individual Laponite layers, hybridized with RhB18 cations, resulting in a height of 1.8–2.0 nm, are rarely observed. Even in 0.2 ppm dispersions, most of the Laponite layers were aggregated. The resulting particles in the LB films are composed of two Laponite layers as explained above in case 3, with corresponding characteristic heights of 3.6 nm. With the addition of a third hydrated Laponite layer, a characteristic height of 5.0 nm was established. Small Laponite layers have a greater tendency to aggregate than the larger layers of natural smectites. Aggregates of two or three Laponite layers are more easily captured by RhB18 molecules at the air-water interface than the larger layers of the natural smectites investigated here. Electrostatic attraction between the cationic RhB18 molecules and Laponite aggregates of two and three layers is thus sufficient to overcome the gravitational forces; much more difficult in the case of clay layers of larger size.

CONCLUSIONS

A comparative study of hybrid LB films consisting of elementary clay mineral layers hybridized with RhB18 cations was performed. The AFM images reveal typical sizes and shapes of the clay mineral layers: laths for hectorite, plates for Wyoming bentonite, a mixture of

Table 2. Characteristic height-distribution maxima and their frequency of occurrence.

Clay	Height (nm)	Occurrence (%)	Height (nm)	Occurrence (%)
Saponite	1.8	40	3.5	60
Laponite	3.6	65	5.0	35
Wyoming bentonite	2.1	40	3.0	60
Hectorite	2.1	40	3.0	60

https://doi.org/10.1346/CCMN.2009.0570604 Published online by Cambridge University Press

laths and plates for saponite, and very small rounded layers of Laponite. The natural clay minerals lead to single layers hybridized with RhB18 and two clay layers hybridized with RhB18. Single Laponite layers are almost absent from the LB films, consisting largely of particles of two or three elementary layers hybridized with RhB18. Particles consisting of two or three clay layers exist in the dispersion in the LB trough and were hybridized by RhB18 at the air-water interface. Such particles may also have been built at the air-water interface. The hybridized monolayer was formed first, therefore, and then a second (hydrated) elementary clay layer and perhaps a third were attached to it. The latter is considered unlikely for two reasons. (1) The probability of such collisions is small and so the two-layer particles should occur less frequently than monolayer particles. (2) If a clay layer had already been hybridized by RhB18, there was no (electrostatic) driving force which would lead to a second elementary clay layer being attached. This can only occur if the amount of RhB18 adsorbed was in excess of the cation exchange capacity of the clay layer to which it is attached.

ACKNOWLEDGMENTS

TS acknowledges support of the Flanders-Hungary bilateral collaboration. JW acknowledges the financial support of K.U. Leuven for a postdoctoral position. The research was supported by the FWO-Flanders, an IAP grant of the Belgian government, CECAT, Long Term Structural Funding-Methusalem Funding by the Flemish Government, and by the Flanders-Hungary bilateral agreement.

REFERENCES

Balnois, E., Durand-Vidal, S. and Levitz, P. (2003) Probing the morphology of laponite clay colloids by atomic force microscopy. *Langmuir*, **19**, 6633–6637.

Beutelspacher, H. and van der Marel, H.W. (1968) *Atlas of Electron Microscopy of Clay Minerals and their Admixtures: A Picture Atlas*. Elsevier, Amsterdam, 333 pp.

Bickmore, B.R., Hochella, M.F., Bosbach, D., and Charlet, L. (1999) Methods for performing atomic force microscopy imaging of clay minerals in aqueous solutions. *Clays and Clay Minerals*, **47**, 573–581.

Bickmore, B.R., Nagy, K.L., Sandlin, P.E., and Crater, T.S. (2002) Quantifying surface areas of clays by atomic force microscopy. *American Mineralogist*, **87**, 780–783.

Bujdak, J. (2006) Effects of layer charge of clay minerals on optical properties of organic dyes. A review. *Applied Clay Science*, **34**, 58–73.

Cadene, A., Durand-Vidal, S., Turq, P., and Brendle, J. (2005) Study of individual Na-montmorillonite particle size, morphology and apparent charge. *Journal of Colloid and Interface Science*, **285**, 719–730.

Čapková, P., Mal, P., Pospíšil, M., Klika, Z., Weissmonová, H., and Weiss, Z. (2004) Effect of surface and interlayer structure on the fluorescence of rhodamine B-montmorillonite: modeling and experiment. *Journal of Colloid and Interface Science*, **277**, 128–137.

Carrado, K.A. and Bergaya, F., editors (2007) Clay-based polymer nano-composites (CPN). CMS Workshop Series vol. **15**. The Clay Minerals Society, Chantilly, Virginia, USA. 278 pp.

Cenens, J. and Schoonheydt, R.A. (1988) Visible spectroscopy of methylene blue on hectorite, laponite B and barasym in aqueous suspension. *Clays and Clay Minerals*, **36**, 214–224.

Klika, Z., Weissmonová, H., Čapková, P., and Pospíšil, M. (2004) The rhodamine B intercalation of montmorillonite. *Journal of Colloid and Interface Science*, **275**, 243–250.

Lindgreen, H., Garnaes, J., Hansen, P.L., Besenbacher, F., Laesgaard, E., Stensgaard, I., Gould, S.A.C., and Hansma, P.K. (1991) Ultrafine particles of North Sea illite/smectite clay minerals investigated by STM and AFM. *American Mineralogist*, **76**, 1218–1222.

Ras, R.H.A., Johnston, C.T., Franses, E.I., Ramaekers, R., Maes, G., Foubert, P., De Schryver, F.C., and Schoonheydt, R.A. (2003) Polarized infrared study of hybrid Langmuir-Blodgett monolayers containing clay minerals. *Langmuir*, **19**, 4295–4302.

Ras, R.H.A., Németh, J., Johnston, C.T., DiMasi, E., Dékany, I., and Schoonheydt, R.A. (2004a) Hybrid Langmuir-Blodgett monolayers containing clay minerals: effect of clay concentration and layer charge density on the film formation. *Physical Chemistry Chemical Physics*, **6**, 4174–4184.

Ras, R.H.A., Németh, J., Johnston, C.T., Dékany, I., and Schoonheydt, R.A. (2004b) Orientation and conformation of octadecyl rhodamine B in hybrid Langmuir-Blodgett monolayers containing clay minerals. *Physical Chemistry Chemical Physics*, **6**, 5347–5352.

Ras, R.H.A., Umemura, Y., Johnston, C.T., Yamagishi, A., and Schoonheydt, R.A. (2007) Ultrathin hybrid films of clay minerals. *Physical Chemistry Chemical Physics*, **9**, 918–932.

Roberts, G.G. (1990) *Langmuir-Blodgett Films*. Plenum Press, New York.

Ruiz-Hitzky, E., Ariya, K., and lvov, Yu. (2008) *Bio-inorganic Hybrid Nanomaterials*. Wiley-VCH, Weinheim, Germany, 503 pp.

Tournassat, C., Neaman, A., Villiéras, F., Bosbach, D., and Charlet, L. (2003) Nanomorphology of montmorillonite particles: estimation of the clay edge sorption site density by low-pressure gas adsorption and AFM observations. *American Mineralogist*, **88**, 1989–1995.

Yariv, S. (2001) Staining of clay minerals and visible absorption spectroscopy of dye-clay complexes. Pp. 463–566 in: *Organo-clay Complexes and Interactions* (S. Yariv and H. Cross, editors). Marcel Dekker, New York.

Zbik, M. and Smart, R.St.C. (1998) Nanomorphology of kaolinites: comparative SEM and AFM studies. *Clays and Clay Minerals*, **46**, 153–160.

(*Received 4 March 2009; revised 30 June 2009; Ms. 291; A.E. S. Petit*)